Available online at www.sciencedirect.com
ScienceDirect
Journal of the European Ceramic Society 29 (2009) 1789–1794
www.elsevier.com/locate/jeurceramsoc

Microstructure and electrical properties of ZnO–Bi_2O_3-based varistor ceramics by different sintering processes

Dong Xu [a,b], Liyi Shi [a,b,*], Zhenhong Wu [a], Qingdong Zhong [b], Xinxin Wu [c]

[a] *Research Center of Nano Science and Technology, Shanghai University, Shanghai 200444, China*
[b] *School of Material Science and Engineering, Shanghai University, Shanghai 200072, China*
[c] *College of Science, Shanghai University, Shanghai 200444, China*

Received 11 July 2008; received in revised form 21 October 2008; accepted 31 October 2008
Available online 6 February 2009

Abstract

The effect of sintering processes, such as open sintering, sintering inside a closed crucible, and sintering within a powder bed, on the microstructure and *V–I* characteristics of ZnO–Bi_2O_3-based varistor ceramics was investigated at sintering temperatures in the range 1000–1200 °C. The results from the experiments showed that the microstructure and electrical properties of the samples varied according to the sintering method and temperature. Optimal values for the electrical characteristics of the varistor ceramics by different sintering processes were obtained when the sintering was conducted at 1100 °C. At the same sintering temperature, the different processes affected the properties differently. At 1000 °C, the samples sintered within a powdered bed showed better electrical properties than those subjected to the other two processes, while at 1100 or 1200 °C, the samples sintered in an open crucible exhibited the best electrical properties.

Keywords: Varistors; ZnO; Sintering; Final microstructure; Electrical properties

1. Introduction

Varistor ceramics are electronic ceramic devices whose function is to limit voltage surges by becoming strongly conducting at a breakdown voltage.[1,2] ZnO-based varistor ceramics play a leading role in making surge protection devices, which are commonly used to protect electric power systems from transient voltages.[3–5] The nonlinear current–voltage characteristic of ZnO-based varistor ceramics is a grain-boundary phenomenon, and the electrical characteristics of the varistor are directly related to the size of the ZnO grain.[6,7] The method of preparation, crystalline size, and homogeneity of the additive are critical for producing good varistor materials. Varistor ceramics with inhomogeneous microstructure can cause a large spread in current–voltage characteristics due to high local currents, which lead to the degradation of the varistor during electrical operation.[1] Varistor ceramics are rather complex, being mainly composed of ZnO to which small amounts of oxides such as Bi_2O_3, Sb_2O_3, Co_2O_3, MnO_2 and Cr_2O_3 have been added.[6] The powder is mixed, then pressed and sintered at higher temperatures to make the dense, final products. The microstructure of the sintered material comprises a matrix of highly conductive ZnO grains with two major secondary phases: a spinel-type phase mainly located at the grain boundaries and triple points, and a Bi-rich phase surrounding the ZnO grains and promoting the formation of potential barriers to electrical conduction at the ZnO homojunctions.[3,8]

In the classical ZnO-based varistor, Bi_2O_3 is used as the varistor-former,[9] thus it is essential for inducing the nonlinearity of the ZnO ceramics.[10] Bi_2O_3 is particularly important since it provides the medium for liquid-phase sintering, enhances the growth of ZnO grains, and affects the stability of the nonlinear current–voltage characteristics of the material. The melting point of Bi_2O_3 is 825 °C. The eutectic temperature of ZnO–Bi_2O_3 is only 740 °C, thus a liquid is formed in the ZnO–Bi_2O_3 specimens below 800 °C. As soon as the eutectic liquid is formed, the weight loss starts to increase. This indicates that the vaporization of Bi_2O_3 starts immediately after the eutectic liquid has been formed.

Peiteado and his co-workers[11,12] used the X-ray fluorescence method to investigate the effect of the area/volume ratio on

* Corresponding author at: Research Center of Nano Science and Technology, Shanghai University, Shanghai 200444, China. Tel.: +86 21 6613 6068; fax: +86 21 6613 6038.
E-mail address: sly0726@163.com (L. Shi).

0955-2219/$ – see front matter © 2008 Published by Elsevier Ltd.
doi:10.1016/j.jeurceramsoc.2008.10.020

the vaporization of Bi in ZnO varistors. To reduce the loss of material, Metz et al.[13] suggested using a new route, in which ceramics are produced by mixing pre-synthesized spinel and pyrochlore phases with the other classical single-oxide additives. Onreabroy et al.[14] have noted that the nonlinear coefficient depended primarily on the sintering temperature, which significantly decreased at higher temperatures, probably due to the volatilization of Bi_2O_3. Weight loss by uncontrolled Bi_2O_3 vaporization is a crucial parameter in the manufacture of varistor ceramics.[15] However, the effects of the sintering process on the electrical properties and vaporization of the Bi_2O_3 in varistor ceramics have seldom been reported.

In this paper, the microstructure and the electrical response of varistor ceramics sintered at differing temperatures and by differing processes were studied in order to obtain a sintering process which can control the vaporization of Bi_2O_3 more effectively.

2. Experimental procedure

2.1. Sample preparation

ZnO–Bi_2O_3-based varistor samples with a nominal composition of 96.5 mol.% ZnO, 0.7 mol.% Bi_2O_3, 1.0 mol.% Sb_2O_3, 0.8 mol.% Co_2O_3, 0.5 mol.% Cr_2O_3, and 0.5 mol.% MnO_2 were used. Reagent-grade raw materials were mixed and homogenized in absolute ethanol media in a polyethylene bowl with zirconia balls for 5 h at 500 rpm by planetary high-energy ball milling. The ratio of balls to the mixed powder was, respectively, 20:1. The slurry was dried at 70 °C for 24 h, it was then pulverized by an agate mortar/pestle and after 2 wt.% polyvinyl alcohol (PVA) binder had been added, it was granulated by sieving through a 100-mesh screen to produce the starting power. The power was uniaxially pressed into discs which were 12 mm in diameter and 2 mm in thickness. The pressed disks were heated in air at 500 °C and for 2 h dwell time to release the binder. Then the disks were sintered in air at 1000–1200 °C (2-h dwell time), at a heating rate of 5 °C/min and then cooled in the furnace. The different processes used to sinter the green pellets are shown in Fig. 1, they were open sintering (OS), sintering inside a closed crucible (CS), and sintering within a powdered bed (PS). The green compacts of OS were placed on a corundum sheet covered with a ZnO powder bed in order to avoid material diffusing into the substrate (Fig. 1a). The green compacts of CS were placed on a corundum sheet covered with a ZnO powder bed, and were sealed into an inverse corundum crucible (Fig. 1b). The green compacts of PS were placed in a corundum crucible, the substrate of the crucible was covered with 99.3 mol.% ZnO and 0.7 mol.% Bi_2O_3 powder, and the same powder was then used to bury the green compacts (Fig. 1c). The detailed sintering schedules are given in Table 1. The sintered samples were lapped and polished to 1.0-mm thickness. The final samples were about 10 mm in diameter and 1.0 mm in thickness.

Table 1
Sintering schedules of samples sintered at different temperatures by different processes.

Sintering processes	Sintering temperature θ (°C)		
	1000	1100	1200
OS	C2A	C2B	C2C
CS	C3A	C3B	C3C
PS	C4A	C4B	C4C

2.2. Measurement of microstructures

To observe the microstructure, sintered ZnO samples were fractured and the fractured surface was coated with gold for examination by a scanning electron microscope (SEM) (JSM-6700F, Japan). The average grain size (G) was determined by the linear intercept method, given by $G = 1.56\,L/MN$, where L is the random line length on the micrograph, M the magnification of the micrograph, and N is the number of the grain boundaries intercepted by lines. The crystalline phases were identified by an X-ray diffractometer (Rigaku D/max 2200, Japan) using Cu Kα radiation. The density, ρ, of the pellets was measured geometrically.

2.3. Measurement of V–I characteristics

The DC current–voltage was characterized by coating silver paste onto both faces of the samples. The silver electrodes (diameter 5 mm) were formed by heating at 600 °C for 10 min. The voltage–current (V–I) characteristics were measured by using a V–I source/measure unit (model CJ1001). The nominal varistor voltages (V_N) (breakdown voltage is the voltage at which the varistor switches from a highly resistive to a highly conductive state) at 0.1 and 1 mA were measured and the threshold voltage V_T (V/mm) (breakdown voltage/unit thickness of varistor ceramic; $V_T = V_N$ (1 mA)/d, where d is the thickness of the sample in mm) and the nonlinear coefficient α ($\alpha = \log(I_{1mA}/I_{0.1mA})/\log(V_{1mA}/V_{0.1mA}) = 1/\log(V_{1mA}/V_{0.1mA})$ according to the equation describing the V–I nonlinearity of the

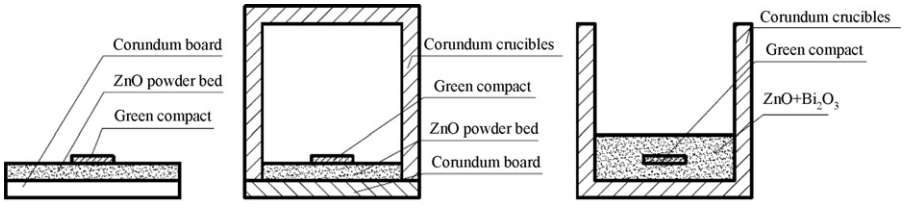

Fig. 1. Sintering processes: (a) OS; (b) CS; (c) PS.

varistor ceramics $I = KV^{\alpha}$, where K is a material constant) were determined. The leakage current (I_L) (the current through the varistor in the pre-breakdown region of the V–I characteristic) was measured at 0.75 V_N (1 mA).[12,14,16–20]

3. Results and discussion

As can be seen from Fig. 2, basically, the density increased and then decreased as the sintering temperature increased, whichever process was being used. Obviously, in all cases, the maximum density was reached at 1100 °C. The densification that occurs during sintering was a main factor in the Bi_2O_3 vaporization, and the higher the sintering temperature, the more the Bi_2O_3 volatilized. When the sintering temperature was above 1000 °C Bi_2O_3 was partially vaporized during the sintering process.[13,21] When the temperature was below 1100 °C, the increase in density due to the densification of the Bi_2O_3 was much more important than the decrease in the density due to the vaporization of Bi_2O_3. However, when the sintering temperature was above 1100 °C, the density of the varistor ceramics clearly decreased because of the vaporization of Bi_2O_3.

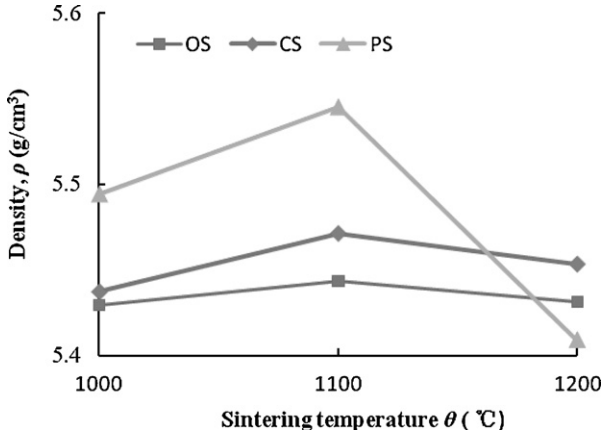

Fig. 2. Density as a function of sintering temperature for different sintering processes.

Fig. 3 shows that the threshold voltage of ZnO–Bi_2O_3-based varistors varies as a function of the sintering temperature. For PS and BS, as the sintering temperature increased, the threshold voltage decreased monotonously. However, the threshold voltage of ZnO–Bi_2O_3 varistors by CS decreased and then increased. For CS, the minimum threshold voltage was reached at 1100 °C, and at 1200 °C the threshold voltage increased slightly,[22] about 13% compared to the minimum.[23] With the increase in sintering temperature, the grain size of the varistor ceramics grew continuously, resulting in the drop in the threshold voltage. However, for CS in the range 1100–1200 °C, the threshold voltage increased again with the increase in sintering temperature, which was different from the OS and PS. When the sintering temperature increases, Bi_2O_3 will volatilize and decompose, the growth of the main crystal phase will be restricted, and yet, the spinel phase, $Zn_7Sb_2O_{12}$, and other secondary phases form and grow. At the same time, these secondary phases gradually solid solved other cations made the ZnO/$Zn_7Sb_2O_{12}$ into an electrically active junction. Therefore, although the number of ZnO/ZnO junctions was reduced because of the growth of ZnO grains, the formation of ZnO/$Zn_7Sb_2O_{12}$ electrical active junctions increased the effective number of grain boundaries, resulting in an increase in the threshold voltage.[22,23]

As shown in Fig. 4, the nonlinear coefficient of the ZnO varistors first increased and then decreased for all three sintering processes, and reached a maximum at 1100 °C. The nonlinear coefficient of the OS and the CS changed as a function of temperature, first increasing and then decreasing. The nonlinear coefficient of the OS was always higher than that of the CS at the same sintering temperature. When sintered at 1000–1100 °C, the nonlinear coefficient for the OS only changed slightly, and when sintered at 1200 °C, it declined sharply, up to 82% compared to the maximum. These variations in the nonlinear properties with sintering temperature are closely related to the Schottky barrier at the grain boundary.[24] At 1000 °C, the grain boundaries began to be wetted,[25] which enhanced the densification of the varistor ceramics. A better microstructural homogeneity–uniform phase distribution would then be obtained as the sintering temperature increased, which triggered an increase in the nonlinear coeffi-

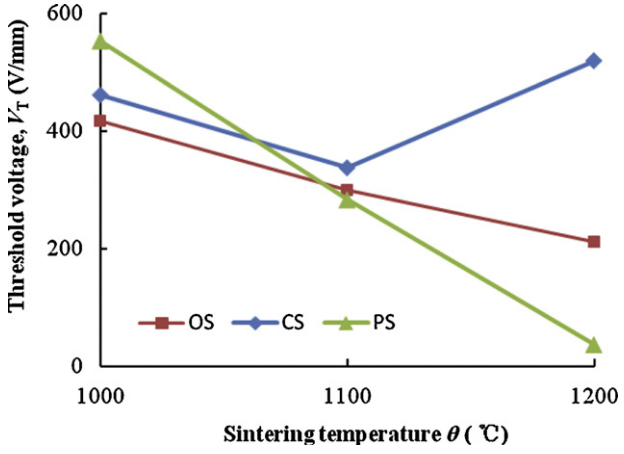

Fig. 3. Threshold voltage as a function of sintering temperature for different sintering processes.

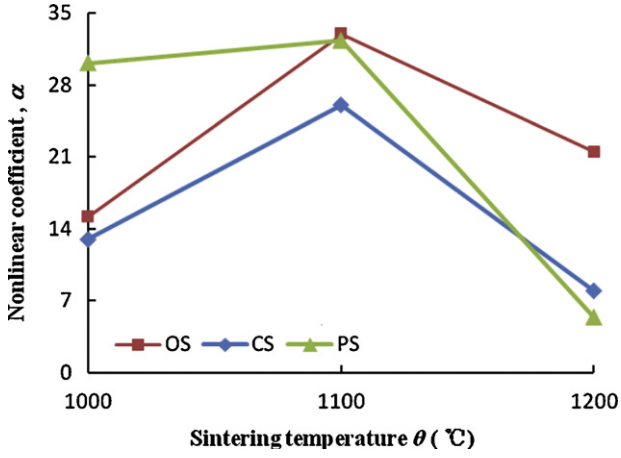

Fig. 4. Nonlinear coefficient as a function of sintering temperature for different sintering processes.

Table 2
Leakage current of samples sintered at different temperatures by different processes.

Sintering processes	I_L (μA)		
	1000 °C	1100 °C	1200 °C
OS	28.50	0.11	11.20
CS	37.00	0.08	108.80
PS	0.44	0.06	222.00

cient. As the sintering temperature was increased further there was a progressive reduction in the nonlinear coefficient, which was attributed to a lowering of the grain boundary barrier height with increased sintering temperature.[18] That is, the lower the barrier height, the worse the nonlinearity is.[26,27] The decrease in the height of the grain boundary barrier was related to the vaporization of Bi_2O_3.

For these three sintering processes, as the sintering temperature increased, the leakage current first decreased and then increased. It reached a minimum at 1100 °C, which suggested that better electrical properties could be obtained at 1100 °C. When the sintering temperature was above 1100 °C, the leakage current increased. To be exact, the leakage current for the PS increased the most, followed by the CS samples and lastly the OS samples. Furthermore, the leakage currents of the varistors sintered at 1200 °C were also higher than those sintered at 1000 °C by PS and CS. In contrast with PS and CS, the leakage current of the varistors sintered at 1200 °C were less than that those sintered at 1000 °C by the OS. Overall, the variation in the leakage current with sintering temperature was opposite to the variation of the nonlinear coefficient. It is believed that the decrease in the leakage current can be attributed to the increase in activation energy (the average energy needed for electrons to overcome the Schottky barrier)[28] and the homogeneous distribution of the limited amount of varistor dopants available in these samples.[20] The Schottky barrier and varistor dopants are related to the Bi_2O_3 content of the varistor ceramics. It is particularly important to realize that the leakage current should be as low as possible for the various applications.[28] The leakage currents of the sintering temperatures for the different sintering processes are summarized in Table 2.

Fig. 5 shows the microstructures of the samples sintered at 1000–1200 °C by OS. It is well known that the microstructure of ZnO–Bi_2O_3 varistor ceramics typically consists of three phases: ZnO grain, spinel, and an intergranular Bi-rich phase as determined by X-ray diffraction (XRD) analysis (see Fig. 6). The microstructures did not differ greatly, except that the grain size with varistor ceramics sintered at 1000–1200 °C by open sintering, and the higher the sintering temperature, the larger the grain size. So did the samples sintered at 1000–1200 °C by CS and PS. The average grain size of the samples sintered at 1000–1200 °C by different processes are presented in Table 3. The different of the grain size was related to the vaporization of Bi_2O_3, which was affected by the different sintering processes. As we know, doping of the ZnO–Bi_2O_3-based varistor ceramics with Sb_2O_3 results in the formation of inversion boundaries (IBs). Recent findings have revealed that IBs play a crucial role via the so-called IBs-induced grain-growth mechanism and microstructural development of varistor ceramics.[20,21,29,30] It is generally known that IBs are related to the Sb_2O_3/Bi_2O_3 ratio,[29] and the amount of Bi_2O_3 is affected by the sintering process.

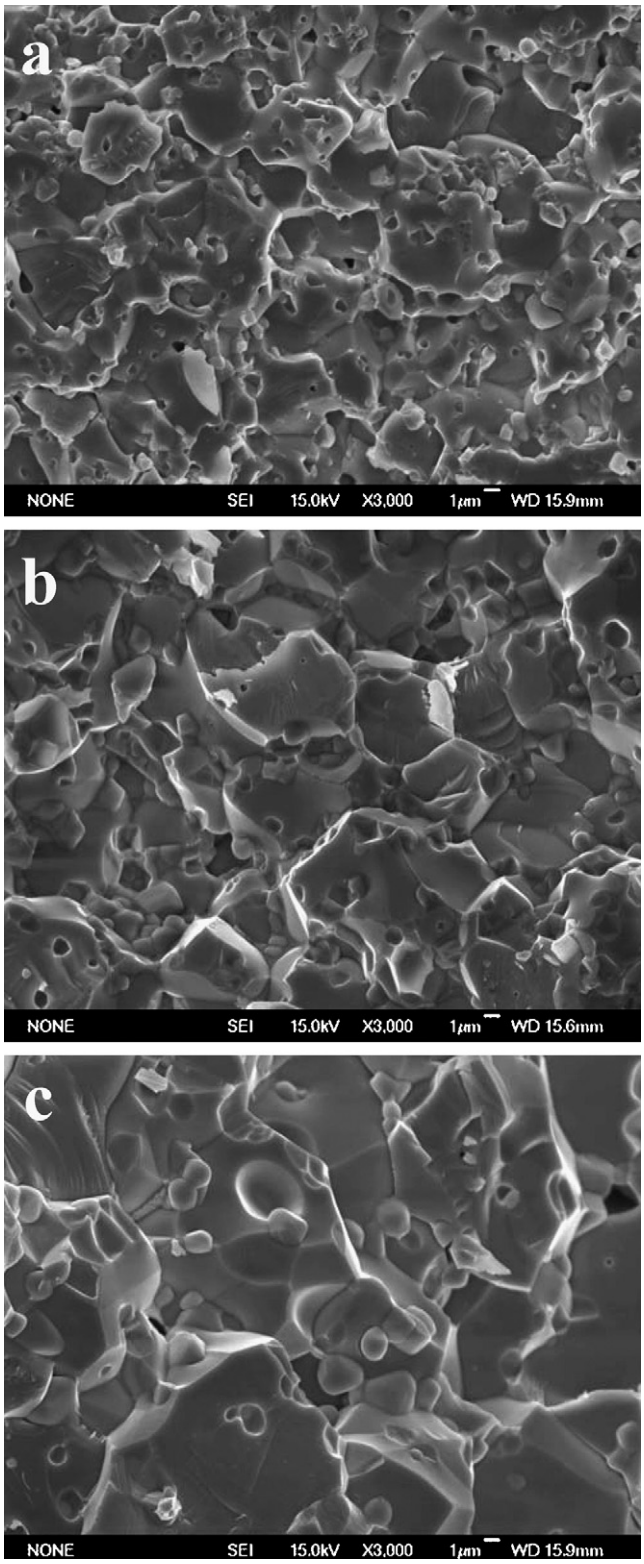

Fig. 5. SEM of ZnO–Bi_2O_3 varistor ceramics sintered at different temperatures by open sintering: (a) C2A; (b) C2B; (c) C2C.

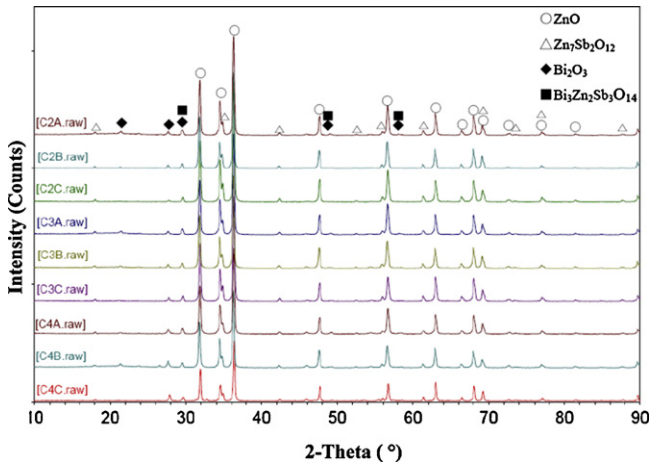

Fig. 6. XRD patterns of ZnO–Bi_2O_3 varistor ceramics sintered at different temperatures by different processes.

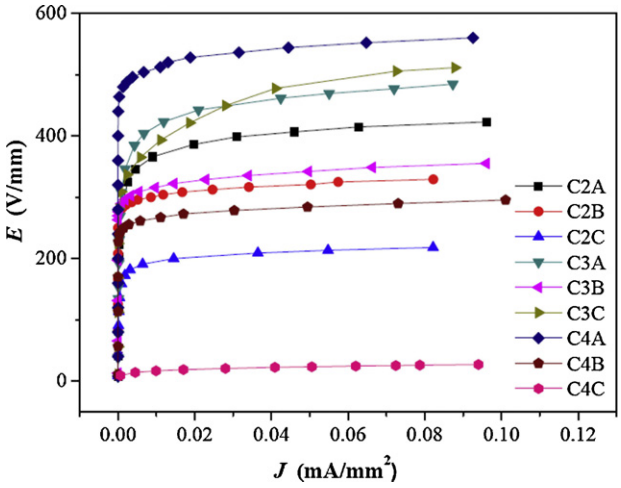

Fig. 7. Electric field–current density (*E–J*) characteristics of ZnO–Bi_2O_3 varistor ceramics sintered at different temperatures by different processes.

Fig. 6 shows the phase composition of the ZnO–Bi_2O_3 varistor ceramics sintered at 1000–1200 °C for 2 h by the different sintering processes. The XRD pattern indicated that ZnO was the main phase, and the additives were not observed because they only account for a small fraction of the overall composition, i.e. less than 1 mol.%, as has been reported previously.[31] The $Zn_7Sb_2O_{12}$ spinel phase and the Bi-rich phase were also identified by XRD. The XRD peak intensities of the Bi-rich phase differ for the three sintering processes. Broadly speaking, at the same sintering temperature, the PS samples had the strongest peak, next were the CS samples, and the OS were weakest. These results showed that PS can control the vaporization of Bi_2O_3 effectively.

Fig. 7 shows the *E–J* characteristics of the ZnO–Bi_2O_3 varistor ceramics sintered at 1000–1200 °C by the different processes. It can be seen from Fig. 7, that when sintered at different temperatures the samples had similar *E–J* curves with a sharp transition from the low current zones to the nonlinear regions. The electrical conduction characteristics are divided into two regions: a linear *E–J* relationship before the critical operation field and a nonlinear *E–J* relationship after the critical operation field. As we know, the sharper the knee of the curves between the two regions is, the better the nonlinear properties are.[24] Only sample C4C shows a much gentler transition, which indicates a poor electrical response. However, it can be forecast that C4C becomes much less pronounced at the knee and the nonlinear properties abruptly reduce. The electrical characterization showed that the differing Bi_2O_3 contents caused serious damage to the varistor characteristics,[20] which can be confirmed by the results of the XRD analysis. This was also confirmed by measuring the varistor functional parameters. Fig. 4 and Table 2 show a low nonlinear coefficient, as well as a very high level of leakage currents in sample C4C. Such poor behavior may be attributed to the Bi_2O_3 content and the grain growth. Fig. 7 also shows that as the sintering temperature increases, the threshold voltages of the samples gradually drop, whatever the sintering process. This can be accounted for by the grain growth. Thus, any excess temperature would only lead to a deterioration in the microstructure and consequently in the electrical properties. In general, the improved electrical characteristics could be attributed to a better microstructural homogeneity–uniform phase distribution and narrower ZnO grain size.[20] As a result, for the three processes (OS, CS, and PS) when sintering at 1100 °C, the electrical characteristics of the varistor ceramics showed their optimal values. At the same sintering temperature, the different sintering processes affected the properties differently. At 1000 °C, the PS samples exhibited better electrical properties than the OS and CS samples, at 1100 or 1200 °C, the OS samples exhibited the best electrical properties.

Table 3
Average grain size of samples sintered at different temperatures by different processes.

Sintering processes	*G* (μm)		
	1000 °C	1100 °C	1200 °C
OS	7.89	8.67	11.93
CS	7.18	10.67	12.35
PS	7.49	10.19	13.22

4. Conclusions

The effects of the three different sintering processes on the microstructure and *V–I* characteristics of ZnO–Bi_2O_3-based varistor ceramics were investigated at temperatures in the range 1000–1200 °C. Basically, the density increased and then decreased as the sintering temperature increased, whichever sintering process was being used. The maximum density for all three processes was reached at 1100 °C. For PS and OS, as the sintering temperature increased, the threshold voltage decreased monotonously. The threshold voltage of ZnO–Bi_2O_3 varistors made by CS first decreased and then increased. The nonlinear coefficient of the ZnO varistors increased and then decreased for all three sintering processes, and reached its maximum at 1100 °C. For all three processes, as the sintering temperature increased, the leakage current basically decreased and then increased, reaching a minimum at 1100 °C. Microstructural

examinations showed that the higher the sintering temperature, the larger the grain size. The experimental results showed that the microstructure and electrical properties of the samples varied in the different sintering methods at different sintering temperatures. The electrical characteristics of the varistor ceramics were at their best in the three sintering processes at 1100 °C. At the same sintering temperature, the different sintering process affected the properties differently. At 1000 °C, the PS samples exhibited better electrical properties than the OS and CS samples, while at 1100 or 1200 °C, the OS samples exhibited the best electrical properties.

Acknowledgments

This work was financially supported by Technical Innovation Team Project of Shanghai Science and Technology Committee (06DZ05902), Leading Academic Discipline Project of Shanghai Municipal Education Commission (J50102) and Academic Leader Program of Shanghai Science and Technology Committee (07XD14014). The authors would like to thank Instrumental Analysis and Research Center of Shanghai University for help with the SEM and XRD measurements.

References

1. Pillai, S. C., Kelly, J. M., Mccormack, D. E., O'Brien, P. and Ramesh, R., The effect of processing conditions on varistors prepared from nanocrystalline ZnO. *Journal of Materials Chemistry*, 2003, **13**(10), 2586–2590.
2. Clarke, D. R., Varistor ceramics. *Journal of the American Ceramic Society*, 1999, **82**(3), 485–502.
3. Anas, S., Mangalaraja, R. V., Poothayal, M., Shukla, S. K. and Ananthakumar, S., Direct synthesis of varistor-grade doped nanocrystalline ZnO and its densification through a step-sintering technique. *Acta Materialia*, 2007, **55**(17), 5792–5801.
4. Duran, P., Capel, F., Tartaj, J. and Moure, C., A strategic two-stage low-temperature thermal processing leading to fully dense and fine-grained doped-ZnO varistors. *Advanced Materials*, 2002, **14**(2), 137–141.
5. Leach, C., Grain boundary structures in zinc oxide varistors. *Acta Materialia*, 2005, **53**(2), 237–245.
6. Bernik, S., Macek, S. and Bui, A., The characteristics of ZnO–Bi_2O_3-based varistor ceramics doped with Y_2O_3 and varying amounts of Sb_2O_3. *Journal of the European Ceramic Society*, 2004, **24**(6),1195–1198.
7. Halls, D. C. and Leach, C., Spectroscopic cathodoluminescence studies of additive free zinc oxide and varistor ceramics. *Acta Materialia*, 1998, **46**(17), 6237–6243.
8. Peiteado, M., Fernandez, J. F. and Caballero, A. C., Processing strategies to control grain growth in ZnO based varistors. *Journal of the European Ceramic Society*, 2005, **25**(12), 2999–3003.
9. Bernik, S., Macek, S. and Bui, A., Microstructural and electrical characteristics of Y_2O_3-doped ZnO–Bi_2O_3-based varistor ceramics. *Journal of the European Ceramic Society*, 2001, **21**(10/11), 1875–1878.
10. Elfwing, M., Osterlund, R. and Olsson, E., Differences in wetting characteristics of Bi_2O_3 polymorphs in ZnO varistor materials. *Journal of the American Ceramic Society*, 2000, **83**(9), 2311–2314.
11. De la Rubia, M. A., Peiteado, M., Fernandez, J. F. and Caballero, A. C., Compact shape as a relevant parameter for sintering ZnO–Bi_2O_3 based varistors. *Journal of the European Ceramic Society*, 2004, **24**(6), 1209–1212.
12. Peiteado, M., De la Rubia, M. A., Velasco, M. J., Valle, F. J. and Caballero, A. C., Bi_2O_3 vaporization from ZnO-based varistors. *Journal of the European Ceramic Society*, 2005, **25**(9), 1675–1680.
13. Metz, R., Delalu, H., Vignalou, J. R., Achard, N. and Elkhatib, M., Electrical properties of varistors in relation to their true bismuth composition after sintering. *Materials Chemistry and Physics*, 2000, **63**(2), 157–162.
14. Onreabroy, W., Sirikulrat, N., Brown, A. P., Hammond, C. and Milne, S. J., Properties and intergranular phase analysis of a ZnO–CoO–Bi_2O_3 varistor. *Solid State Ionics*, 2006, **177**(3/4), 411–420.
15. Kim, C. H. and Kim, J. H., Microstructure and electrical properties of ZnO–ZrO_2–Bi_2O_3–M_3O_4 (M = Co, Mn) varistors. *Journal of the European Ceramic Society*, 2004, **24**(8), 2537–2546.
16. Bernik, S. and Daneu, N., Characteristics of ZnO-based varistor ceramics doped with Al_2O_3. *Journal of the European Ceramic Society*, 2007, **27**(10), 3161–3170.
17. Brankovic, Z., Brankovic, G., Bernik, S. and Zunic, M., ZnO varistors with reduced amount of additives prepared by direct mixing of constituent phases. *Journal of the European Ceramic Society*, 2007, **27**(2/3), 1101–1104.
18. Leach, C., Ling, Z. and Freer, R., The effect of sintering temperature variations on the development of electrically active interfaces in zinc oxide based varistors. *Journal of the European Ceramic Society*, 2000, **20**(16), 2759–2765.
19. Peiteado, M., Fernandez, J. F. and Caballero, A. C., Varistors based in the ZnO–Bi_2O_3 system: microstructure control and properties. *Journal of the European Ceramic Society*, 2007, **27**(13–15), 3867–3872.
20. Bernik, S., Brankovic, G., Rustja, S., Zunic, M., Podlogar, M., Brankovic, Z. and Microstructural, compositional aspects of ZnO-based varistor ceramics prepared by direct mixing of the constituent phases and high-energy milling. *Ceramics International*, 2008, **34**(6), 1495–1502.
21. Lao, Y. W., Kuo, S. T. and Tuan, W. H., Effect of Bi_2O_3 and Sb_2O_3 on the grain size distribution of ZnO. *Journal of Electroceramics*, 2007, **19**(2/3), 187–194.
22. Cheng, P. F., Li, S. T. and Alim, M. A., Soft core behavior in ZnO–Bi_2O_3-based varistors containing oxides of Ce and Gd. *Physica Status Solidi A—Applications and Materials Science*, 2007, **204**(3), 887–899.
23. Zhang, J., Cao, S., Zhang, R., Yu, L. and Jing, C., Effect of fabrication conditions on *I–V* properties for ZnO varistor with high concentration additives by sol–gel technique. *Current Applied Physics*, 2005, **5**(4), 381–386.
24. Nahm, C. W., The effect of sintering temperature on electrical properties and accelerated aging behavior of PCCL-doped ZnO varistors. *Materials Science and Engineering: B*, 2007, **136**(2/3), 134–139.
25. Leach, C. and Vernon-parry, K., The effect of sintering temperature on the development of grain boundary traps in zinc oxide based varistors. *Journal of Materials Science*, 2006, **41**(12), 3815–3819.
26. Nahm, C. W., Effect of sintering time on varistor properties of Dy_2O_3-doped ZnO–Pr_6O_{11}-based ceramics. *Materials Letters*, 2004, **58**(26), 3297–3300.
27. Nahm, C. W., Influence of sintering time on electrical and dielectric behavior, and DC accelerated aging characteristics of Dy^{3+}-doped ZnO–Pr_6O_{11}-based varistors. *Materials Chemistry and Physics*, 2005, **94**(2/3), 275–282.
28. Nahm, C. W. and Park, C. H., Microstructure, electrical properties, and degradation behavior of praseodymium oxides-based zinc oxide varistors doped with Y_2O_3. *Journal of Materials Science*, 2000, **35**(12), 3037–3042.
29. Bernik, S., Daneu, N. and Recnik, A., Inversion boundary induced grain growth in TiO_2 or Sb_2O_3 doped ZnO-based varistor ceramics. *Journal of the European Ceramic Society*, 2004, **24**(15/16), 3703–3708.
30. Daneu, N., Recnik, A. and Bernik, S., Grain growth control in Sb_2O_3-doped zinc oxide. *Journal of the American Ceramic Society*, 2003, **86**(8), 1379–1384.
31. Zhang, D., Fu, H., Shi, L., Fang, J. and Li, Q., Carbon nanotube assisted synthesis of CeO_2 nanotubes. *Journal of Solid State Chemistry*, 2007, **180**(2), 654–660.